jet INTL JOURNAL OF ELECTRONICS AND TELECOMMUNICATIONS, 2010, VOL. 56, NO. 3, PP. 209–214
Manuscript received July 10, 2010: revised September, 2010.
DOI: 10.2478/v10177-010-0027-y

Improvement of the Microwave Imaging System by Deconvolution of the Antenna Pulse Response

Marek Bury, Yevhen Yashchyshyn, and Jozef Modelski

***Abstract*—In the paper a microwave imaging system and its algorithm of image reconstruction from the raw measurement data were briefly introduced. Authors observed that pulse responses of the antennas used in the system have similar duration to the measurement pulse and therefore also contribute to the limits of system resolution. Paper presents a simple method that improves the system performance by additional deconvolution of the antenna pulse responses. Method was verified experimentally.**

***Keywords*—Microwave imaging, antenna pulse response, deconvolution.**

I. Introduction

UTILIZATION of the pulses having ultra wide frequency band (UWB) in microwave imaging systems enables possibility of obtaining great resolution as well as taking benefits from the microwaves' penetrating ability [3], [14]. Such solutions are applicable in a wide range of domains including high resolution ground [15] and wall [8], [18] penetrating radars, medical [6], [5], [17] and security systems[12], [13], to mention just a few.

Short duration of the measurement pulses gives opportunity to perform time analysis and eliminate some of the unwanted signals simply, by limiting the analysis to the time window centered one the time of arrival of the wanted signal. Any interference outside the window becomes then irrelevant [12]. Nevertheless, application of ultra wideband signals imposes also a number of problems. One of them is the fact that the shape of the ultra wideband pulse is easily distorted during the transmission through microwave components. Transmitting and receiving antennas are devices that are critical. Pulse response of the antenna may be even several times longer [1] than the UWB pulse itself. Thus the convolution of the transmitted signal with pulse response of two antennas entirely alters pulse shape and may lead to serious decrease of the UWB system performance. This effect is easy to observe in imaging systems [2], [19], simply by making comparison of images obtained using antennas that have different pulse response [2]. The purpose of this paper is to demonstrate how the performance of the microwave imaging system may be improve by deconvolution of the pulse response of the antenna.

II. Microwave Wideband Imaging System

A. Measurement Setup

Let us consider UWB pulse imaging system based on time of arrival (TOA) approach. A block diagram of applied measurement setup is presented in Fig. 1. It consists of:

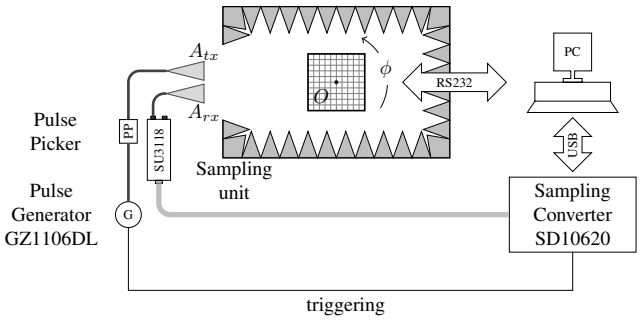

Fig. 1. Measurement setup for time domain, single channel imaging system.

- short pulse generator G with pulse picker (PP),
- sampling converter (SD10620 made by Geozondas);
- sampling unit (SU3118, made by Geozondas);
- personal computer PC, controlling the measurement procedure;
- revolving platform, on which the object under test is located;
- transmitting and receiving antennas.

Measurement procedure is controlled by the personal computer PC. It communicates with sampler (USB interface), controls the revolving (RS232 interface) platform, stores measurement results and finally calculates the image. Sampler adjusts the parameters of time window (duration, number of samples) according to the settings sent by PC, triggers the generator to repeat a number of pulses and so as to acquire dense sampling of reflected signal. It should be stressed that acquired samples are not originated from the same single pulse but from the whole sequence of pulses repeated – one after another – with 1 MHz repetition frequency.

The measurement procedure is simple:

1) Initial state. The angle of platform rotation is equal to zero;
2) PC send the command to the sampler to start measurement;
3) Sampler triggers generator and acquires vector of samples;
4) PC requests samples and stores them in the hard disk;
5) PC checks whether measurements have been performed for all angles.
6) if NO then it causes the platform to rotate by 1° and procedure is repeated from the step 2;
7) if YES then procedure is over.

M. Bury, Y. Yashchyshyn, and J. Modelski are with the Institute of Radioelectronics, Warsaw University of Technology, Nowowiejska 15/19, 00-665 Warsaw, Poland (e-mail: {M.Bury; E.Jaszczyszyn; J.Modelski}@ire.pw.edu.pl).

The result of measurement procedure is a matrix $\mathbf{s}[m,n]$ of signals acquired for whole range of angles of platform rotation. It is a matrix of signals' samples, with one dimension (m) corresponding to time (precisely to the number of the sample in the time window of signal observation) and the other (n) to the angles of the platform rotation.

B. Algorithm of Image Reconstruction

Algorithm of image reconstruction in the present imaging system is described in detail in [2] and [4]. It consists in iterating through the picture pixel by pixel and calculating the intensity. The intensity is being determined by comparing the measurement result against the theoretical (according to the assumed model) prediction of the delay of the pulse reflected from the object located at the coordinates corresponding to the pixel. Most generally, it includes following steps:

1) for given coordinates (x_i, y_i) corresponding to the pixel P_i, a vector of delays $\Delta\tau_i(\phi_n)$ for subsequent angles ϕ_n of platform rotation is calculated;
2) the delay of the $\Delta\tau_i(\phi_n)$ is used to calculate the number $m_i[n]$ of the respective sample in the matrix of raw measurement data, for given angle of rotation ϕ_n;
3) intensity $\mathbf{I}(x_i, y_i)$ of the pixel corresponding to coordinates (x_i, y_i) is proportional to the sum of the samples corresponding to the calculated delays for subsequent angles of platform rotation:

$$\mathbf{I}(x_i, y_i) \sim \sum_{n=1}^{N} \mathbf{s}[m_i[n], n]. \tag{1}$$

Assuming simple geometrical model of the measurement and neglecting the differences in altitudes of the antennas and the revolving platform, it is possible to calculate the vector of delays according to following formula:

$$\begin{aligned}\Delta\tau_i = &\frac{1}{c}\cdot\sqrt{(x_t - x_i(\phi_n))^2 + (y_t - y_i(\phi_n))^2)} + \\ &+ \frac{1}{c}\cdot\sqrt{(x_r - x_i(\phi_n))^2 + (y_r - y_i(\phi_n))^2)} + \\ &- \frac{1}{c}\sqrt{x_t^2 + y_t^2} - \frac{1}{c}\sqrt{x_r^2 + y_r^2},\end{aligned} \tag{2}$$

where: (x_t, y_t) denotes coordinates of the transmitting antenna, (x_r, y_r) – coordinates of the receiving antenna, c – the speed of light and $(x_i(\phi_n), y_i(\phi_n))$ – coordinates (x_i, y_i) after rotation of the platform by angle ϕ_n. Those coordinates can be calculated by substitution to the simple geometrical formulas:

$$\begin{cases} x_i(\phi) = x_i \cdot \cos(\phi) - y_i \cdot \sin(\phi) \\ y_i(\phi) = x_i \cdot \sin(\phi) + y_i \cdot \cos(\phi). \end{cases} \tag{3}$$

C. Measurement Signal

A waveform of measurement signal is presented in Fig. 2a), while Fig. 2 shows its spectrum. The width of the pulse defined at -3 dB is approximately $\Delta t_{3dB} = 30$ ps, which imposes lower limit for the imaging system resolution ie. approximately 0.5 cm, according to the well known formula [9], [11]:

$$\Delta r = c \cdot \frac{\Delta t_{3dB}}{2}. \tag{4}$$

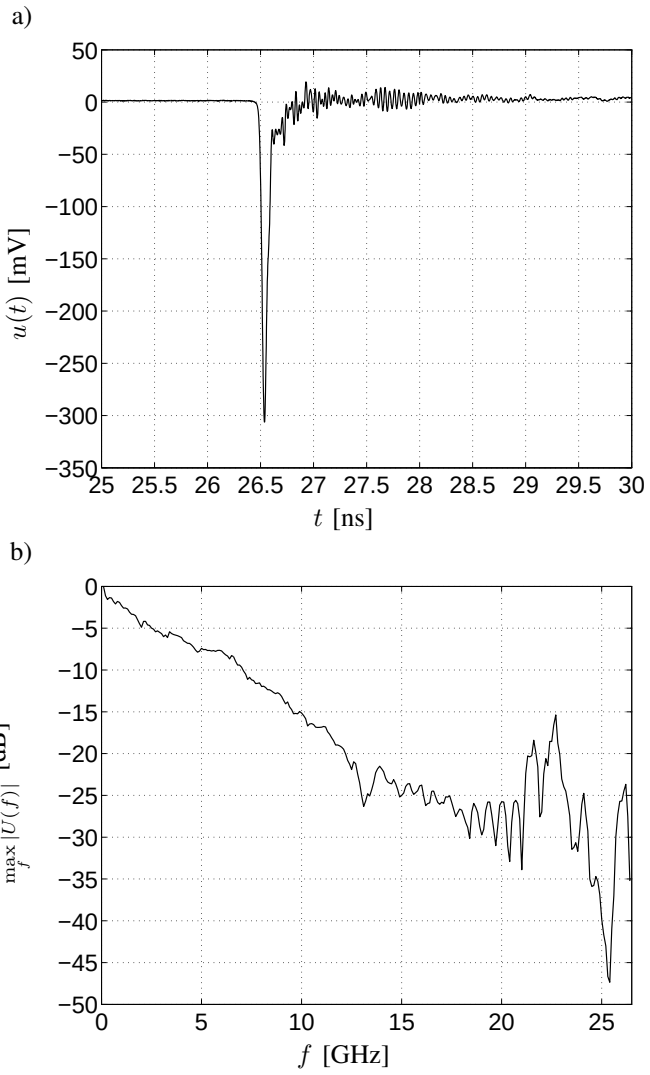

Fig. 2. Measurement pulse: a) waveform, b) amplitude spectrum.

The spectrum of the pulse occupies frequency bandwidth from DC to approximately 16 GHz and that is the range that should be covered by the antennas. Since no antenna is capable of transmitting DC, a signal is inevitably high pass filtered. Reasonable lower limit of the antenna frequency band for this application appears to be 2 GHz.

III. Antenna Pulse Response

A model of radio link based on the antenna pulse response is described in [10], [16] while detailed information about measurement procedures can be found in [16], [2]. For the scope of this paper it is enough to conclude that in the open space model (true enough in anechoic chamber in which the measurement setup is located) and for the copolar operation, the relation between the waveform of the voltage fed to the input port of the transmitting antenna and the output port of the receiving antenna complies to formula:

$$u_{rx}(t) = u_{tx}(t) \star h_{tx} \star F(t, r) \star h_{rx}, \tag{5}$$

where: r denotes the distance that signal travels, $F(t)$ is a certain waveform that depends on the r, while $h_{tx}(t)$ and

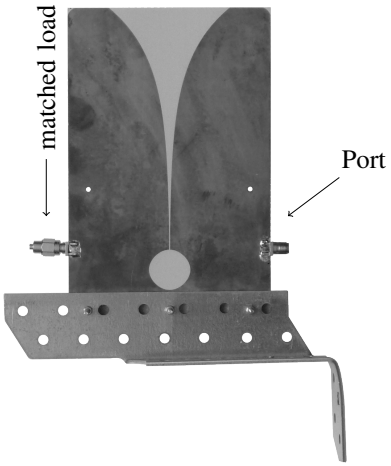

Fig. 3. Planar Vivaldi antenna (receiving antenna in the microwave imaging system).

Fig. 4. TEM horn antenna П6-23(transmitting antenna in microwave imaging system).

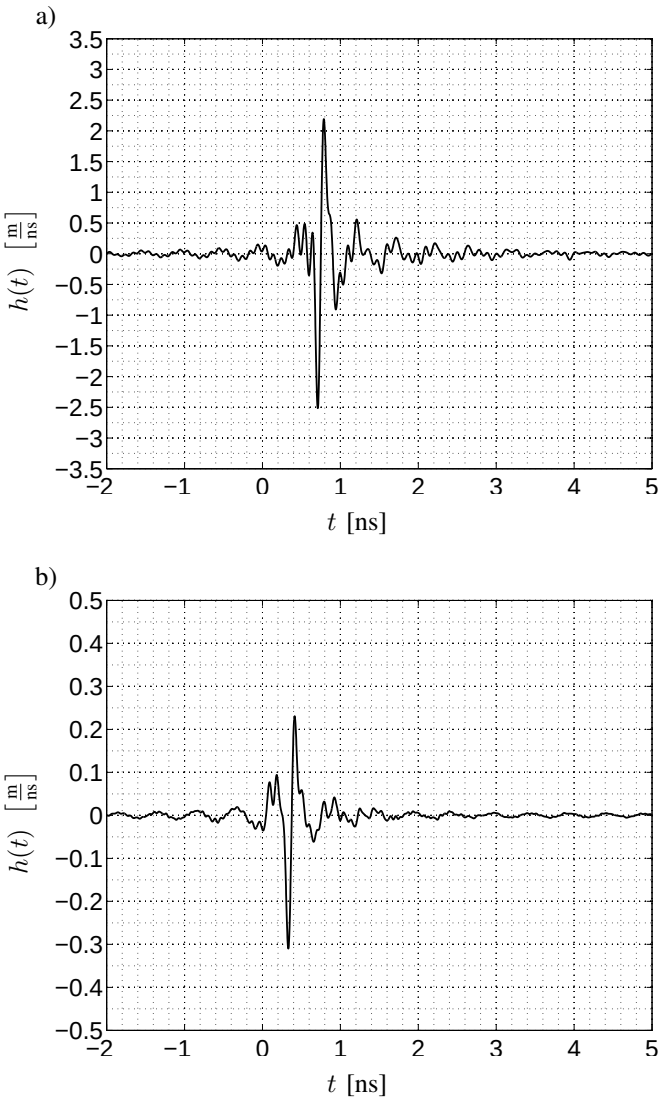

Fig. 5. Pulse response measured in frequency band: $2 \div 10$ GHz: a) the TEM horn П6-23, b) the planar Vivaldi antenna.

$h_{rx}(t)$ denotes pulse response of the transmitting and receiving antenna, respectively.

From (5) it is clear that the received waveform is no shorter than the convolution of the pulse responses of transmitting and receiving antennas. Actually, the length of the received waveform would be equal to the length of $h_t x(t) \star h_r x(t)$ if the measurement pulse ie. $u_{rx}(t)$ was an ideal Dirac pulse $\delta(t)$ and greater otherwise (which obviously is the case, concerning fig 2a). Therefore the pulse response of the antenna may be as well a factor limiting the microwave imaging system resolution.

Antennas used in microwave imaging system are presented in Fig. 3 and Fig. 4.

Fig. 4 presents the transmitting antenna. It is a TEM horn having narrow beam, high gain and short (Fig. 6a and Fig. 5a) pulse response. However its large dimensions make it quite difficult to use. Receiving antenna was a planar Vivaldi antenna, presented in Fig. 3. It is more compact but has significantly wider beam and slightly longer pulse response (Fig. 6a and Fig. 5a).

Pulse responses of both antennas used in the microwave imaging system have been measured according to the three antenna technique described in [2]. The method requires band-pass filtration corresponding to the bandwidth of the antenna under test. Since the term bandwidth is rather ambiguous when it comes to the UWB antenna the measurements were performed in two frequency bandwidths: $2 - 10$ GHz (Fig. 5) and $1 - 18$ GHz (Fig. 6).

In figs 5 and 6 one can see that the amplitude of pulse response of the receiving antenna is nearly ten times lower while the duration (at 3 dB) of the receiving antenna pulse response is approximately twice longer than the duration of the pulse response of the transmitting antenna.

From the results of measurements (figs 5 and 6) of the pulse responses of the antennas used in the imaging system it is clear that applying the deconvolution procedures to the

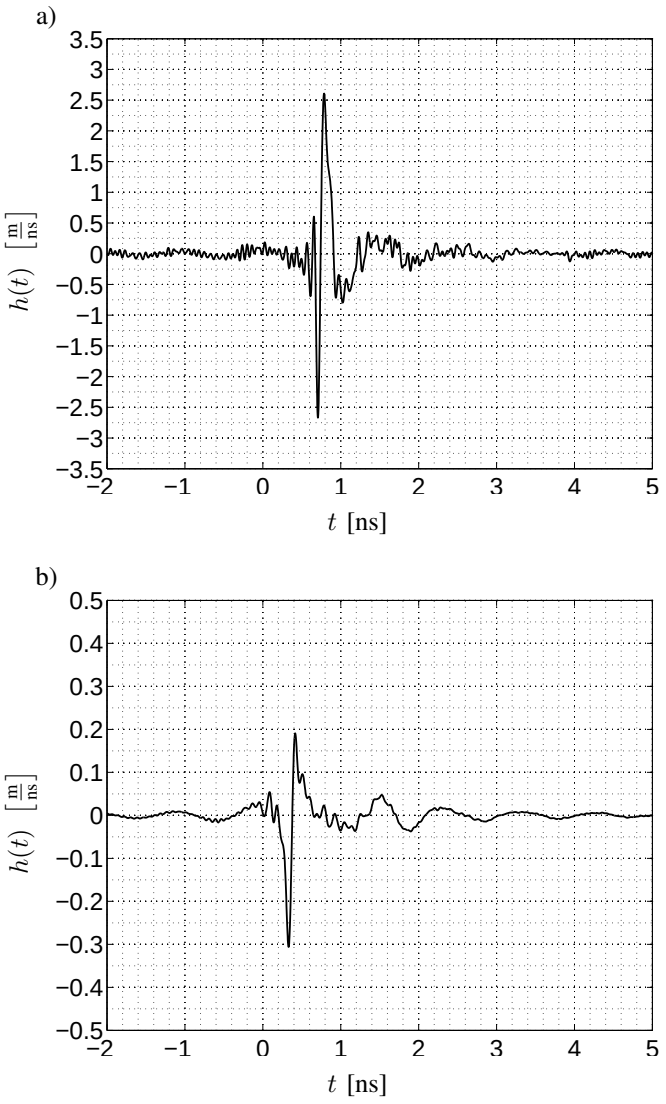

Fig. 6. Pulse response measured in frequency band: $1 \div 18$ GHz: a) the TEM horn П6-23, b) the planar Vivaldi antenna.

raw measurement data should help to improve the system resolution. This is due to the fact that the length of the pulse responses is comparable to the length of the measurement pulse (Fig. 2a).

IV. Deconvolution Procedure

The conclusion of the previous section was verified in simple experiment. The deconvolution procedure was quite simple:

1) for given row $r_n(t)$ of the raw measurement data matrix $\mathbf{s}[m,n]$ and a waveform to be deconvoluted $w(t)$ Fourier transforms are calculated: $R(\omega)$ and $W(\omega)$;
2) the Fourier transform of the row after deconvolution $R_{d,n}(\omega)$ is calculated by simple division:

$$R_{d,n}(\omega) = \frac{R_n(\omega)}{W(\omega)}; \tag{6}$$

3) the waveform $r_{d,n}(t)$ of the row after deconvolution is calculated by inverse Fourier transform;
4) the procedure is repeated for all rows of the raw measurement data matrix and in result gives deconvoluted measurement data matrix $\mathbf{s_d}[m,n]$.

Above-mentionted deconvolution procedure has two weak points. The first is step 2 in which measurement data are divided by the values that at certain frequencies may be close to zero. Therefore both measurement data and the deconvoluted data need to be filtered so as to eliminate samples for which deconvolution procedure produces large uncertainty. Otherwise, after transformation to the time domain, those uncertain samples would produce significant additional noise.

The second weak point is the fact that in the simple radio link model (5) additional noise and interferences are not taken into account (similar phenomenon is described in the context of channel equalization in [7]). Most of them are introduced to the signal after it is transmitted by the transmitting antenna and therefore they are not convoluted with its pulse response. Consequently, inverse filtering may lead to uncontrolled errors resulting from transforming those additional interferences. Authors found it advisable to make two deconvolution related experiments and try deconvoluting two different waveforms from the raw measurement data. First waveform was naturally the pulse response of the receiving antenna $h_{rx}(t)$, while the second was measured pulse response of the radio link $h_{tot}(t)$ comprising both antennas and measurement cables. Both waveforms were measured prior to obtaining raw measurement data matrix.

Fig. 7. Reproduction of the Walter CP88.

V. Measurement Results

A. Object Under Test

Object under test (OUT) is related rather with security applications of the microwave imaging systems. Though it was selected for it has well defined and easy to recognize shape and simultaneously comprises a number of details. Observation of those details on the resulting images make image comparison easier.

OUT is presented in Fig. 7. It is a replica of the firearm Walter CP88. It was measured without its case, simply put into an open plastic box on the revolving platform.

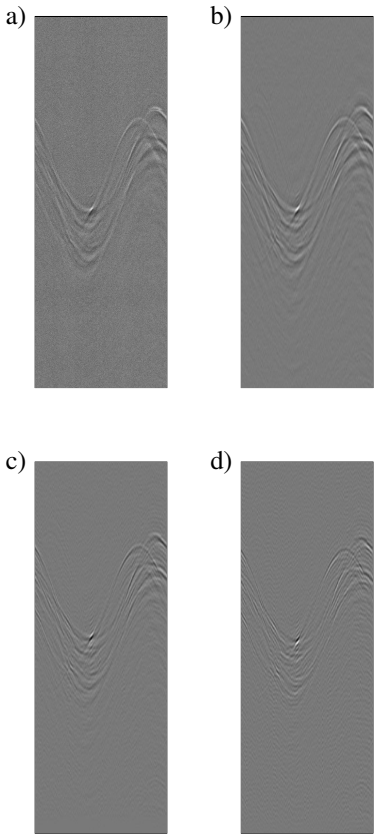

Fig. 8. Raw measurement data (echogram): a) pre-processed; b) pre-processed and bandpas filtered ;c) pre-processed after deconvolution of the receiving antenna's pulse response; d) pre-processed and after deconvolution of the waveform $h_{tot}(t)$.

B. Raw Measurement Data

Raw measurement data acquired for 720 angles of observation of the OUT (angle step was $0.5°$) are presented in Fig. 8a). Since deconvolution procedure also included bandpass filtration, in Fig. 8b) the same data are shown, but with the same filtration as is applied in deconvolution procedure. Figure 8 c) presents measurement data after deconvolution of the receiving antenna pulse response $h_{rx}(t)$ and Fig. 8 d) presents the same data after deconvolution of the waveform $h_{tot}(t)$ mentioned in section IV;

It is clear that the hodographs (traces of the reflecting points) visible in Fig. 8 became sharper after the deconvolution but it is difficult to tell how much it is going to influence the reconstructed images.

C. Reconstructed Images

All data matrices presented in Fig. 8 were used to reconstruct images. Results are presented in figs. 9 and 10.

Comparing Fig. 9 (without deconvolution) against Fig. 10 (with deconvolution) leads to the obvious conclusion that deconvolution improves the images despite the imposed bandpass filtration. Contours of the firearm in images reconstructed from the data after deconvolution are fairly sharper.

It is more difficult to tell which of the pictures presented in Fig. 10 is better. In authors' opinion, in image a) it is possible

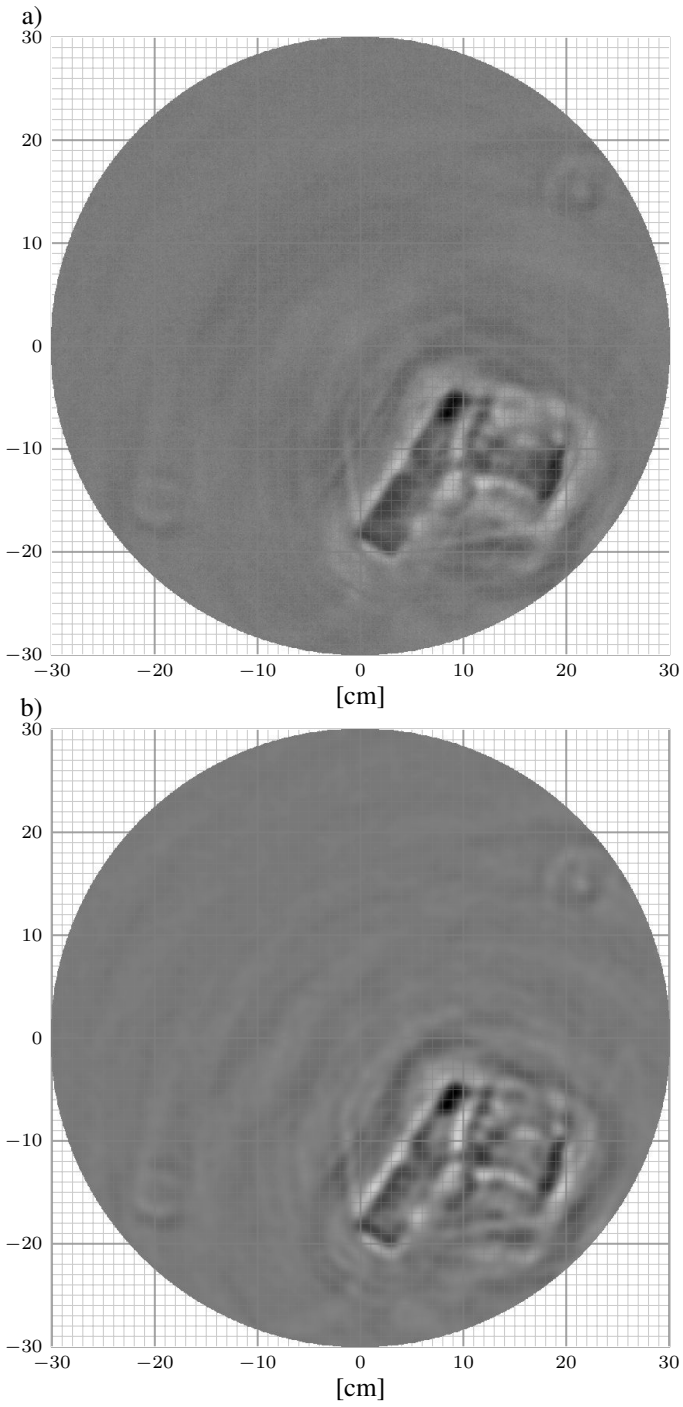

Fig. 9. Image obtained from measurement data: a) without bandpass filtration b) with bandpass filtration.

to recognize the trigger guard as opposed to image b) and therefore it is better. Nevertheless, differences appeared to be rather insignificant.

VI. Conclusions

In the paper a microwave imaging system and its algorithm of image reconstruction from the raw measurement data were briefly introduced. Authors observed that pulse responses of the antennas used in the system have similar duration to

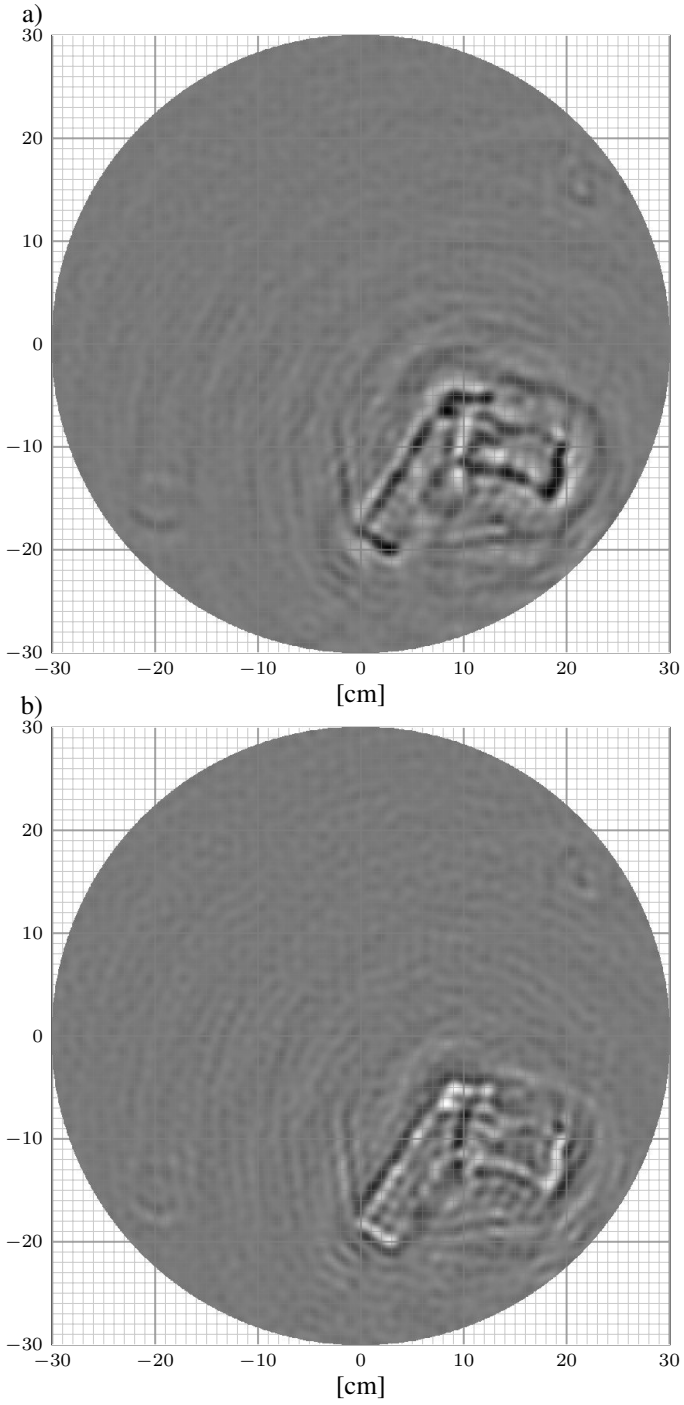

Fig. 10. Image obtained from the raw measurement data: a) after deconvolution of the pulse response of the receiving antenna; b) after deconvolution of the waveform $h_{tot}(t)$.

the measurement pulse and therefore also contribute to the limits of system resolution. That leads to the conjecture that additional deconvolution of the antenna pulse responses may improve the imaging system performance. Knowing that inverse filtration applied to deconvolute the pulse response of the transmitting antenna may introduce additional distortions to the data authors verified their conjecture for two cases. One was deconvolution of the pulse response of the receiving antenna alone and the second was the deconvolution of the pulse response of the whole radio link comprising cables and both antennas. Experiment was done with an exemplary object under test which was a replica of the firearm Walter CP88. Analysis of the images reconstructed from the raw measurement data and the data after deconvolution allowed authors to conclude that the approach proved to be helpful to improve system performance and that the deconvolution of the pulse response of the receiving antenna only gave slightly better result.

REFERENCES

[1] M. Bury and Y. Yashchyshyn, "Pulse Response of UWB Antenna: Meaning and Simple Measurement Procedure," in *2nd European Conference on Antennas and Propagation*, Edinburgh, UK, Nov. 11-16, 2007.

[2] M. Bury, "Obrazowanie obiektw na podstawie wielopunktowej akwizycji mikrofalowych sygnaw szerokopasmowych," Ph.D. dissertation, Warsaw University of Technology, 2009.

[3] M. Bury and Y. Yashchyshyn, "Short-pulse ISAR coherent penetrating radar," R. S. Romaniuk, Ed., vol. 6159, no. 1. SPIE, 2006, p. 61591R.

[4] M. Bury, Y. Yashchyshyn, and J. Modelski, "A Simple Approach for Elimination of Fixed Objects' Reflections in UWB Imaging System," in *The International Conference on "Computer as a Tool"*, Warsaw, Poland, Sep. 9–12, 2007, pp. 299–302.

[5] S. K. Davis, H. Tandradinata, S. C. Hagness, and B. D. Van Veen, "Ultrawideband microwave breast cancer detection: a detection-theoretic approach using the generalized likelihood ratio test," *IEEE Trans. Biomed. Eng.*, vol. 52, no. 7, pp. 1237–1250, Jul. 2005.

[6] S. Davis, B. Van Veen, S. Hagness, and F. Kelcz, "Breast tumor characterization based on ultrawideband microwave backscatter," *IEEE Transactions on,Biomedical Engineering*, vol. 55, no. 1, pp. 237 –246, jan. 2008.

[7] S. G. Glisic, *Advanced Wireless Communications, Second Edition (Second Edition)*. John Wiley & Sons, Chichester 2007.

[8] S. Hantscher, A. Reisenzahn, and C. Diskus, "Through-wall imaging with a 3-d uwb sar algorithm," *IEEE Signal Processing Letters*, vol. 15, pp. 269 –272, 2008.

[9] M. Kolawole, *Radar Systems, Peak Detection and Tracking*. Elsevier, 2002.

[10] J. Kunish and J. Pamp, "UWB radio channel modellng considerations," in *Proc. of ICEAA03*, Turin, Sep. 2003, pp. 497–498.

[11] N. Levanon and E. Mozeson, *Radar Signals*. John Wiley & Sons, 2004.

[12] B. Levitas and J. Matuzas, "UWB radar high resolution ISAR imaging," in *Second International Workshop Ultrawideband and Ultrashort Impulse Signals*, Sep. 19–22, 2004, pp. 228–230.

[13] ——, "Evaluation of UWB ISAR image resolution," in *European Radar Conference*, Paris, Oct. 6–7, 2005, pp. 89–91.

[14] J. Modelski, M. Bury, and Y. Yashchyshyn, "Short-pulse Microwave Imaging System," in *5th International Conference on Microwave Electronics: Measurements, Identification, Applications*, Dec. 13–15, 2005, pp. 31–36.

[15] Y.-J. Park, S.-B. Cho, K.-H. Kim, and D.-G. Youn, "Development of an ultra wideband ground penetrating radar (UWB GPR) for nondestructive testing of underground objects," in *IEEE Antennas and Propagation Society International Symposium*, vol. 2, Jun. 20–25, 2004, pp. 1279–1282.

[16] W. Sörgel and W. Wiesbeck, "Influence of the Antennas on the Ultra-Wideband Transmission," *Journal on Applied Signal Processing*, no. 3, pp. 296–305, 2005.

[17] E. Staderini, "Uwb radars in medicine," *IEEE Aerospace and Electronic Systems Magazine*, vol. 17, no. 1, pp. 13 –18, jan 2002.

[18] Y. Yang, C. Zhang, and A. Fathy, "Development and implementation of ultra-wideband see-through-wall imaging system based on sampling oscilloscope," *IEEE Antennas and Wireless Propagation Letters*, vol. 7, pp. 465 –468, 2008.

[19] Y. Yashchyshyn and M. Bury, "Time Characterization Versus Classical Antenna Parameters in Ultra-wide Frequency Bands," in *International Conference Modern Problems of Radio Engineering, Telecommunications, and Computer Science*, Lviv – Slavsk, Ukraine, Feb. 28– Mar. 4 2006, pp. 497–498.